Earth Systems and Environment
https://doi.org/10.1007/s41748-020-00147-9

ORIGINAL ARTICLE

Impacts of Potential Sea-Level Rise on Tidal Dynamics in Khor Abdullah and Khor Al-Zubair, Northwest of Arabian Gulf

Ali Abdulridha Lafta[1,2] · Samer Adnan Altaei[2] · Noori Hussain Al-Hashimi[1]

Received: 5 October 2019 / Accepted: 28 January 2020

Abstract
According to recent studies, sea-level rise (SLR) not only increases the coastal flooding probability but also may change the characteristics of tidal systems in coastal waterbodies. To investigate such changes in Khor Abdulla and Khor Al-Zubair, a two-dimensional depth-averaged model was applied. The calibration and validation were performed through the comparison of model results with measurements of water level and flow velocities in particular sites within model domain. SLR scenarios of 0.25, 0.5, 0.75, and 1 m were simulated. The simulation results indicate that the response of the principal tidal constituents was spatially nonuniform and exhibited a nonlinearity with SLR scenarios. However, the M_2 amplitude decreases in most locations with SLR, with the most reduction occur in the upper reaches of the study area, while S_2 and N_2 amplitudes display a slight increase in a most sites along KA and KZ. Similarly, the amplitudes of K_1 and O_1 experience to a notable decrease in most locations when sea level rises. Additionally, there is a reduction in constituents' phases with SLR scenarios. The decrement in constituents' phases indicates that these waves will arrive earlier when sea level rises due to the nature of tidal wave propagation and their dependency on the water depth. Furthermore, the magnitude of the tidal currents also displays a spatially irregular response to SLR with a noticeable shift in the time of peak flood and ebb current velocities in many locations, while the direction of the currents remains unchanged at most sites of the study area.

Keywords Sea-level rise · Tidal dynamics · Harmonic analysis · Tidal constituents · Arabian gulf · Mike21

1 Introduction

Global warming has manifested its impact on the world oceans in several ways, including changes in ocean heat contents, ocean acidification, and deoxygenation, leading to variations in oceanic circulation, ocean chemistry, sea levels rising (SLR), as well as changes in the diversity and abundance of marine species (Wernberg et al. 2014). Global warming increases sea level through two factors: first, melting of glaciers and ice sheets, and the melt water flows into the ocean to increase sea level. Second, heat expansion, warm water takes up more space than colder water, increasing the volume of water in the ocean (IPCC 2013). The calculation and analyzing the rate of SLR are carried out through three methods, past tide gauge records, satellite altimetry data, and air–sea coupling model forecasting (Kuang et al. 2014). The tide gauge data show that the sea level rose from 1870 to 2004 by 195 mm, with a twentieth century rate of SLR of 1.7 ± 0.3 mm/y, and accelerated by 0.013 ± 0.006 mm/y^2 (Church and white 2006). While the satellite altimetry data have shown that global mean sea level has been rising at a rate of 3 ± 0.4 mm/y since 1993 with accelerating rate at 0.084 ± 0.025 mm/y^2 (Nerem et al. 2018). However, according to the fourth Intergovernmental Panel on Climate Change report (IPCC 2007), the projected SLR at the end of the twenty-first century will be about 0.79 m, with 0.2 m representing an inaccuracy in measurements due to the accelerated melting rate of ice sheets, while the fifth IPCC report refers to sea level can be rise more than 10 cm of IPCC fourth report estimates (IPCC 2013). But, according to some studies, these values are very optimistic that confirms a significant acceleration in the rate of SLR compared to these estimations. However, according to the study of Mengel et al. (2016) in which many computational tools were used to predict SLR, sea level at the end of the

✉ Ali Abdulridha Lafta
ali.lafta@uobasrah.edu.iq

[1] Department of Physics, College of Education for Pure Science, University of Basra, Basra, Iraq

[2] Department of Marine Physics, Marine Science Center, University of Basra, Basra, Iraq

Published online: 03 March 2020

twenty-first century is projected to be 0.57 to 1.31 m, unless greenhouse gas emissions are reduced as soon as possible. Furthermore, the projected SLR will be about 2 m by the end of the twenty-first century as proposed by Nicholls et al. (2011) and Sriver et al. (2012).

Coastal areas represent the most densely populated around the world and SLR will be the most damaging factor for those living in low-lying coastal regions with significant social and economic repercussions (IPCC 2013). The most important problems that coastal areas are expected to face due to SLR are the loss of low-lying coastal lands, accelerated erosion along the coast, salt intrusion into lakes and estuaries, degradation of coastal ecosystems, rise in nearby groundwater levels, and the impact on the benthic ecology (Haines 2008; Xie et al. 2015; Testut et al. 2016). SLR also has a significant impact on tidal systems, as suggested by many studies, a slight rise in sea level over the past few decades has affected tidal systems as a response to this rise (Woodworth et al. 2009; Müller et al. 2011), and it is expected that this effect will continue in the case of sea-level rise in the future due to the propagation characteristics of the tidal wave and affected by the depth of water, especially in shallow waters (Pickering et al. 2012;Pelling and Green 2013; Pelling et al. 2013a, b; Carless 2016; Kuang et al. 2016; Passeri et al. 2016; Du et al. 2018; Harker et al. 2019; Surya et al. 2019). Furthermore, any variations in the tidal systems will lead to significant changes in the hydrodynamic properties as a response to this effect, impacting on current velocities, tidal ranges, circulation patterns of water, sediment transport processes and morphological evolution and associated ecosystem of the tidal basin over the long-term, navigation, and infrastructure near the coast (Pelling et al. 2013a, b; Valentim et al. 2013; Arns et al. 2015; Kuang et al. 2016; Suh 2016).

Khor Abdullah (KA) and Khor Al-Zubair (KZ) situated at the northwest tip of Arabian Gulf represent the most important part of Iraqi marine water, used for many purposes such as navigation, industries, fisheries, oil transportation and recently introduced in oil production processes in southern Iraq (SOC 2014). The tidal dynamics are mainly responsible for the hydrodynamics characteristics at KA and KZ, and SLR in the Arabian Gulf may change the tidal characteristics of KA and KZ. However, the estimation of SLR rates in the Arabian Gulf is confirmed by several studies. Sultan et al. (1995) have shown by analysis the tide data in the Arabian Gulf for the period of 11 years (1980–1990), the presence of a positive trend of the surface level of the Gulf reach 2.1 mm/y. Sultan et al. (2000) pointed out that when analyzing the tide data for a period of 15 years for the Saudi coast on the Arabian Gulf, the existence of a rise in the surface level of the Gulf up to 1.7 mm/y, which is consistent with the global rise in sea level, according to the results of this study. While the study of Alothman and Ayhan (2010) point out that by using tide data for 26 years along the coasts of Saudi Arabia and Bahrain to the presence of sea-level rise in the west of the Arabian Gulf up to 2.42 ± 0.21 mm/y. Also, the study of Alothman et al. (2014), show that using the tide data for a period of 28.7 years (1979–2007), there is a rise in sea level in the northwestern part of the Arabian Gulf by 1.5 ± 0.8 mm/y, which consistent with the global estimation of rising in sea level (Church and White 2011). However, the latest study presented by Siddig et al. (2019), using tide data for 29 years covering the period 1979–2008 at seven stations along the west coast of the Arabian Gulf in Saudi Arabia, showed an increase in sea level, with a maximum value of 3.4 ± 0.98 mm/y. Yet, there are limited studies that dealt with the impact of SLR in the northern part of the Arabian Gulf. Shahidi et al. (2015) studied the effect of SLR by 0.3, 0.6, and 0.9 m on the distribution of salinity in Bahmanshir estuary in western Iran, which flows into the northern Arabian Gulf using the Mike11 model, and they point out that increasing the depths by SLR lead to increase of the amount of water entering the estuary during the tidal phase, which in turn leads to an increase of salt intrusion towards the upper reaches of the estuary. Alsahli and Al-hasem (2016) showed that by assuming SLR by 0.5, 1, 1.5, and 2 m on the Kuwait coasts based on remote sensing techniques and digital elevation models (DEM), the northern regions are more vulnerable to flooding, especially the Warba and Bobian islands in addition to the west coast of Kuwait bay in the case of a rise of 0.5 m. While in our study area, only one study has been carried out by Al-Mahmood et al (2018) about the effect of SLR on the southern part of Iraq, by assuming a rise of 0.3, 0.5, and 1 m, based on DEM data, to identify the areas that at risk of flooding in south of Iraq. Yet, there is no study of the impacts of potential SLR on tidal dynamics of KA and KZ, so the current study represents the first attempt to investigate the impacts of SLR by assuming several scenarios and track the possible changes in the tidal dynamics in KA and KZ. To address this objective, tidal levels and currents field measurements were conducted. Then, a two-dimensional tidal model based on Mike21 is developed. The simulation assumed the SLR scenarios of 0.25, 05, 075, and 1 m to cover possible changes in tidal dynamics over this century. These scenarios are used to assess the response of the five principle tidal constituents and currents field to SLR.

2 Materials and Methods

2.1 Study Area

The Iraqi marine waters represent the most estuarine part of the northwestern of the Arabian Gulf and consist of Shatt AL-Arab estuary and several open lagoons such as Khor Al-Kafka, Khor Al-Amaya and Khor Abdullah (Al-Mahdi

et al. 2009). Khor Abdullah is shallow water with the depths ranged from 7 to 14 m and averaged about 10 m and characterized by its funnel shape and surrounded by the Al-Faw peninsula on the east bank and Bobian island on the other, with wide intertidal zones on its banks (Mohamed et al. 2002). The total length of Khor Abdulla channel about 40 km and width of about 17 km at its confluence with the Arabian Gulf and reduces to about 6.5 km south of Warba island when forming Khor Bobian that connects it with Khor Al-Subia and Khor Al-Zubair which extend towards the northwest direction of Iraqi territory (Fig. 1). Moreover, Khor Al-Zubair channel is an extension of Khor Abdulla and they connected through Khor Shytana. The average area in Khor Al-Zubair that covered by water is approximately 60 km^2 and with a mean tidal range exceed 4 m at spring tide (Al-Ramadhan 1988). The depth of the navigation channel in KZ ranges between 10 and 20 m. The northern part of the KZ is composed of several irregular shallow tidal lagoons with complex geometry that formed a characteristic shaped like tree fronds. In 1983, an artificial canal (Shatt A-Basrah canal) was opened that connects the Euphrates river with KZ. In 1993, Shatt Al-Basrah canal connection with Euphrates river was closed, and a new connection made with MOD (Main Outfall Drain) at about 10 km from the head of the canal (Fig. 1). The MOD canal which contains the water of the drained regions of the Euphrates basin is agricultural water drainage through Shatt Al-Basrah canal then discharged towards the Arabian Gulf through KZ and KA (Lafta et al. 2013). In the last years, the inflow of MOD was converted towards the Iraqi marshlands and in the present time, a very little amount of water (do not exceed 10 m^3/sec) discharged in the Shatt Al-Basrah canal. The climate of the region is characterized by an arid desert climate with two distinct seasons, the summer which is a hot and long and winter that represent a cold and rainy season. There are two types of prevailing winds in the area, northwest winds, which causes dust storms in the summer, and locally known as Al-Shammal which is a characteristic of the region and southeast winds mostly during autumn and winter that is relatively warm and moist and occasionally brings rainy clouds (Zakaria et al. 2013).

2.2 Data Collection

To fulfill the study objectives, many kinds of data are used, which includes water level measurements, bathymetry, flow velocity, and wind speed and direction. The water level measurements at three sites are carried out, the first situated at the inlet of KA (ST1 in Fig. 1), these data for the year 2018 was obtained from the tide gauge installed by Daewoo Engineering and constructing company. The water level data in Umm Qasar town (ST2) are collected by installing a Valeport TideMaster Portable Tide Gauge with pressure sensor for the year 2018, while the water level data at Khor Al-Zubair port station (ST3) is acquired from Khor Al-Zubair Port Authority. All these data are hourly records and references to the local chart datum (Lowest Low Water) in this region. It is worthy to mention that there are interruptions in recordings of water level for 20 days through April/ 2018 in Khor Al-Zubair port station. Bathymetric data were acquired from many sources, marine science center/ Basrah university surveys conducted in 2005 (MSC 2005), Admiralty

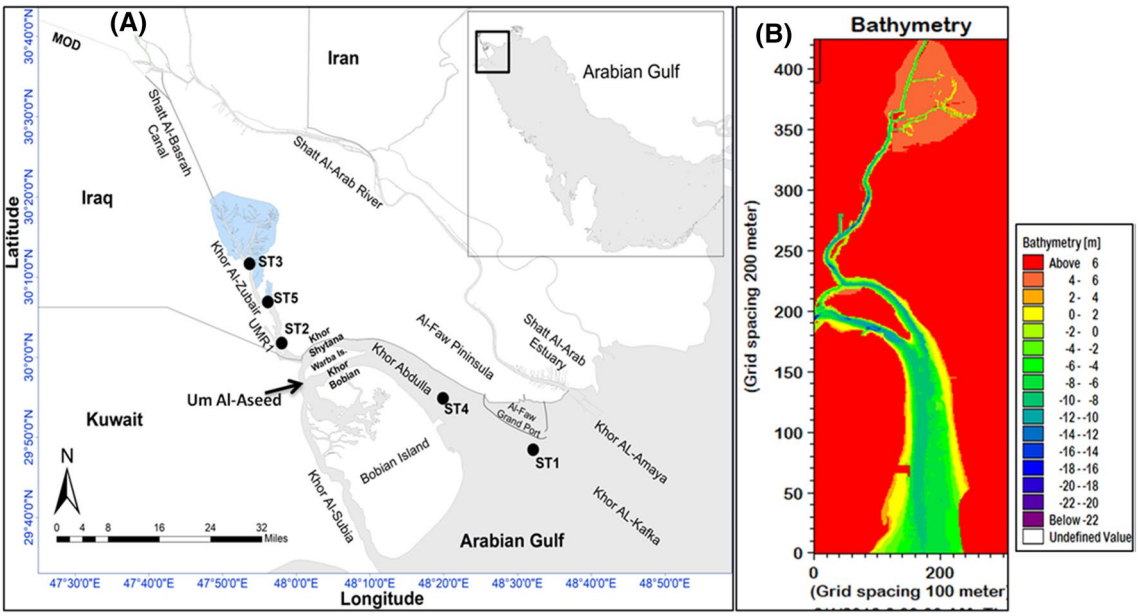

Fig. 1 Geographical location (**a**) and bathymetric characteristics (**b**) of the study area

charts No. 1235 modified by British Hydrographic Office in 2010, and the surveyed that carried out by Tatweer Office to South Oil company/ Iraq (SOC 2014). Topographical data on the tidal flats and surrounding lands are obtained from the digital elevation model of Shuttle Radar Topography Mission (STRM) (earthexplorer.usgs.gov) using GIS extracted tools. Horizontal coordinates are given in easting and northing projection coordinates systems, Universal Transverse Mercator (UTM) and the water depths were referenced to the local chart datum (CD). Furthermore, the flow velocity measurements were carried out using an Acoustic Doppler Current Profile (ADCP) at two sites (ST4 and ST5 in Fig. 1), with an hourly record on a full tidal cycle is utilized on the 16th to 17th of March and on the 22nd to 24th April 2018. Metrological data including the wind speed and direction were obtained from the weather station installed by Daewoo Engineering and constructing company at KA inlet (ST1 in Fig. 1).

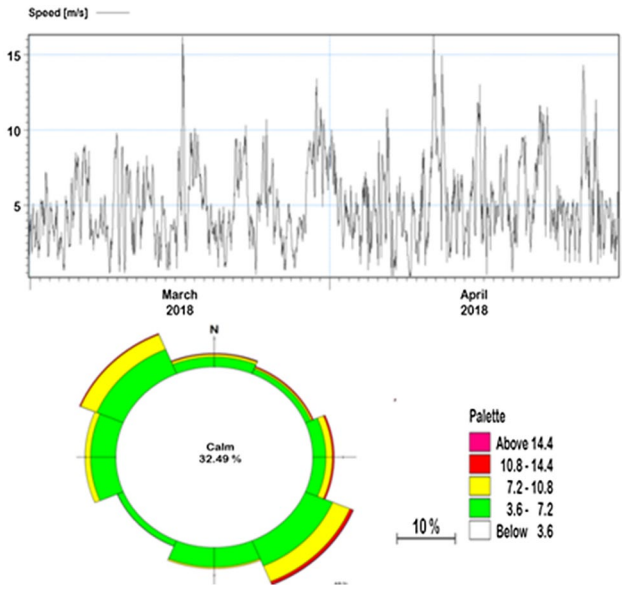

Fig. 2 Wind speeds and wind rose in study area

2.3 Model Setup

Mike21, a depth-averaged two-dimensional modeling system, is used to study the impact of potential SLR on tidal dynamics in KA and KZ. A hydrodynamic (HD) model represents the core of this model, it simulates the water level fluctuations and flows in response to many of forces, such as tides, metrological effects and density-driven flows arising from temperature and salinity variations, in open seas, estuaries, lagoons, bays, and coastal areas. The governing equations and model details can be found in the Mike21 scientific documentation (DHI 2007).

The bathymetry of the computational domain of study area is derived from the bathymetry data as we mentioned earlier. It is divided by a rectangular grid with spatial discretization 100 × 200 m, with 310 × 425 grid points through x and y directions, respectively. There are three open boundaries in the domain, first is located at KA inlet, second is located at Khor Bobian inlet at Umm Al-Aseed, and lastly open boundary located at KZ upper reaches, near its confluence with Shatt Al-Basrah canal (Fig. 1). The model was forced by the realistic water level data as well as wind fields which applied as a constant over the whole domain and varying with time as illustrated in Fig. 2. At first open boundary, the water level records at ST1 was utilized. While, due to a lack of water level records at second boundary, the water level data by Total Tide software, which is a predictive tidal tool proposed by the United Kingdom of Hydrographic Office, was used. Furthermore, there are no available measurements at upper open boundary, so to obtain a time series of data in this location, the output result from the Shatt Al-Basrah model implement by Mike11 model is used (Lafta et al. 2013). This model is well calibrating of the year 2009, so some modulations are added to implement it in current conditions, first the south open boundary of this model is extended to be at ST2 that include entire KZ, and water level measurements at ST2 are used as a boundary condition, and the flow of Shatt Al-Basrah at current time put in to be equal to 10 m^3/s, then the model was run and calibrate and validate through water level and flow velocities at ST3 and St5, respectively, and the results from this calculation is used to feed the mathematical model of KA and KZ. The initial condition of the model is selected to be a cold start, i.e. surface elevation and velocity are set to be zero at the beginning of the simulation at all grid points of the model domain.

The model was run for two months, starting from 1st March to 30th April of 2018. To ensure the high stability of model performance, a time step of 5 s is set up which leads to a maximum courant number of 0.729. However, for the regions that suffer from successive flooding and drying during the tidal cycle such as tidal flats, the flooding and drying depths have a pronounced effect on the HD model estimations. The Mike21 recommended range of flooding depth are 0.001 to 0.02 m and for drying depth is 0.002 to 0.04 m (Filipova et al. 2012), so the value of 0.005 m was used for flooding and 0.06 m for drying depths which are considered as a good approximation in reproducing the hydrodynamics parameters throughout the studying area. The effect of winds fields (wind speed and direction which measured at a 10 m over sea level, Fig. 2) on the HD model calculations are taken into account by including the wind shear stress, with a wind drag coefficient of 0.0024.

To ensure the best performance of the HD model, the computed result of water level and flow velocities are directly compared with field measurements. Two statistical parameters were used to this purpose, Root Mean Square

Error (RMSE) and Nash–Sutcliffe Efficiency Coefficient (NSE) (Nash and Sutcliffe 1970),

$$\mathrm{RMSE} = \sqrt{\frac{\sum_{i=1}^{N}(M_i - C_i)2}{\mathrm{N}}} \tag{1}$$

$$\mathrm{NSE} = 1 - \frac{\sum_{i=1}^{N}\left(M_i - C_i\right)^2}{\sum_{i=1}^{N}\left(M_i - \bar{M}_i\right)^2}, \tag{2}$$

where M_i is a sum of measured values, C_i is the sum of simulated values, N is a number of values, and M_i is an avarege of measured values. To obtain the optimum performance of the HD model, a various sensitivity analysis was carried out through varying the calibration parameters like the bottom friction coefficient and eddy viscosity. The bottom friction (Manning number M) of 50 $m^{1/3}$/sec and a Smagorinsky constant for Eddy viscosity of 0.3 were chosen to get the best matching between measured and simulated values. The data of March/2018 was used in the calibration of the model. The comparisons between the simulated and observed water levels at ST2 and ST3 are shown in Fig. 3, and between simulated and measured flow velocities at ST4 and ST5 are shown in Fig. 4.

Furthermore, the validation of the model was achieved by utilizing the measurements of April/2018. Figure 5 shows the comparison between measured and simulated water levels at ST3 and ST2, while Fig. 6 illustrates the comparison between simulated and measured flow velocities. Table 1 summarizes the values of RMSE and NSE for the calibration and validation periods.

A satisfactory agreement has been achieved between measured and simulated for water levels and flow velocities. The model also reproduced the spring-neap cycles through the simulation period. generally, the model reasonably well reproduced the surface level and flow velocities and given acceptable results that can be used for future assessments of hydrodynamic characteristics in the study area.

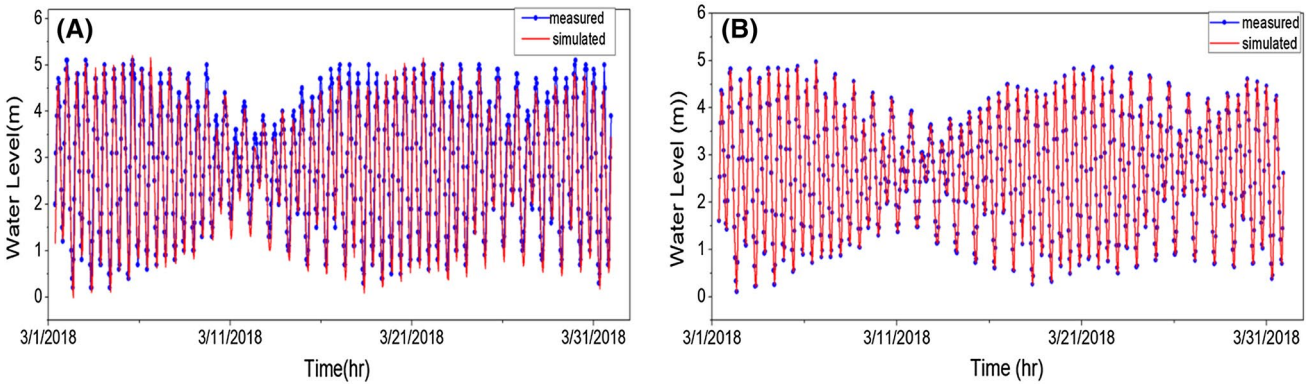

Fig. 3 Comparison between measured and simulated water level (**a**) at station ST3, (**b**) at ST2

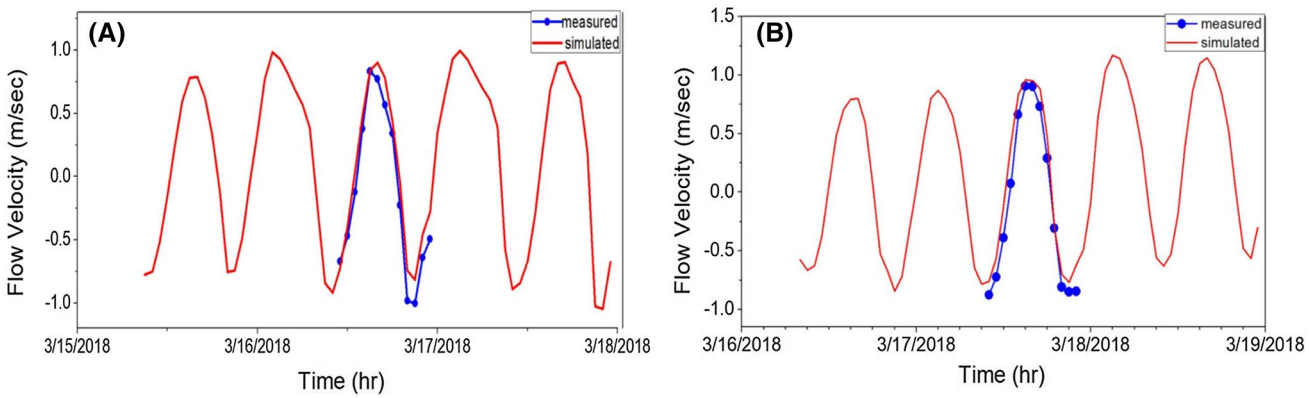

Fig. 4 Comparsion between measured and simulated flow velocities (**a**) at station ST5, (**b**) at ST4

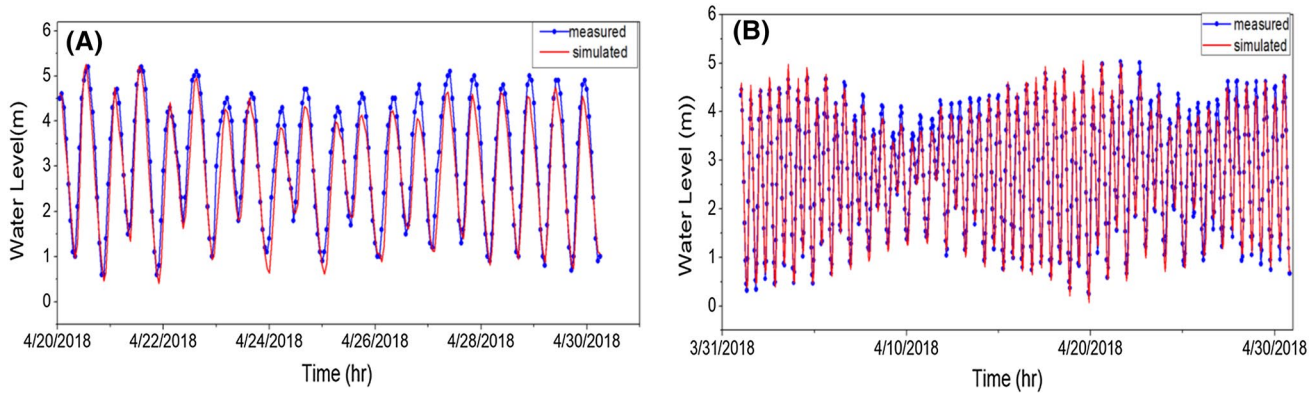

Fig. 5 Comparsion between measured and simulated water level (**a**) at station ST3, (**b**) at ST2

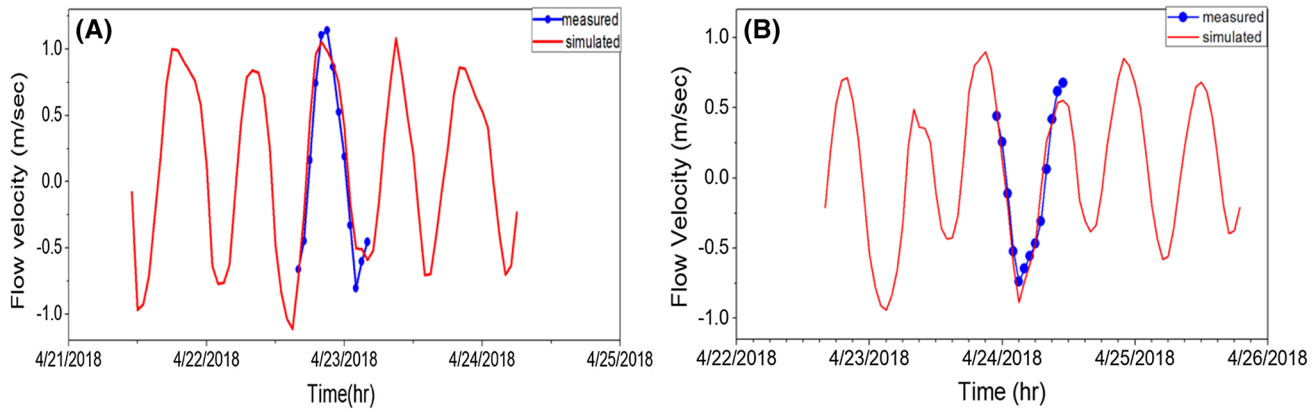

Fig. 6 Comparsion between measured and simulated flow velocities (**a**) at station ST5, (**b**) at ST4

Table 1 Root mean square error and Nash–Sutcliffe efficiency coefficient for the calibration and validation periods

Stations	Calibration period		Validation period	
	RMSE	NSE	RMSE	NSE
ST2 (water level)	0.26 m	0.997	0.27 m	0.99
ST3 (water level)	0.45 m	0.991	0.47 m	0.98
ST4 (flow velocity)	0.17 m/s	0.95	0.12 m/s	0.97
ST5 (flow velocity)	0.15 m/s	0.96	0.32 m/s	0.99

3 Results and Discussion

Understanding of SLR impacts on tidal systems is a fundamental issue to anticipate any future ecosystem shifts and to adapt, present and modify appropriate management strategies in coastal water bodies. However, numerical experiments were designed to investigate the impacts of SLR on tidal dynamics in KA and KZ, using the calibrated and validated hydrodynamics model. The SLR scenarios were assumed to be 0.25, 0.5, 0.75, and 1 m relative to the base scenario (SLR = 0 m). The SLR scenarios were implemented in the Mike21 HD model by uniformly deepened the bathymetry for the entire computational domain by these SLR values, as conducted by several studies (Siqueira 2011; Gong et al. 2012; Pelling et al. 2013a, b; Li et al. 2016; Harker et al. 2019). Every scenario was run for 2 months (March and April of 2018), and the results of these scenarios were compared with the base scenario.

3.1 Tidal Dynamics in Khor Abdullah and Khor Al-Zubair

Sea level data records in ST1, ST2, and ST3 are used to study the characteristics of the tidal wave by harmonic analysis using Matlab World Tide (Boon 2007), and to examine the main components of tides in the study area. The results indicated that the five principle astronomical tidal constituents (K_1, O_1, M_2, S_2, and N_2) explain about 93% of the total variances of water level in the KA and KZ, M_2 was the main contributor to the total variation of water levels, followed

by K_1, S_2, O_1, and N_2. The results revealed that there is a gradual increase in the tidal amplitude coming from Arabian Gulf when it propagates further towards the upper reaches of KZ due to the convergence nature of the study area, with a significant increase in the amplitudes of the principle semi-diurnal constituents (M_2, S_2, and N_2) and a slight increase in the amplitudes of the principle diurnal constituents (K_1, O_1). However, the percentage of increase in the amplitude of M_2 constituent reaches about 48% in ST2 and 68% in ST3 relative to its amplitude in ST1, while the percentage of increase for the rest constituents were 43%, 64.4% for S_2; 34%, 40% for N_2; 6%, 11% for K_1; and 3.5%, 4.1% for O_1 in ST2 and ST3, respectively, compared to their amplitudes in ST1. The tide in KA and KZ followed a similar rhythm and the form number was 0.68, 0.48 and 0.44 in ST1, ST2, and ST3, respectively. However, according to the tidal classification by Defant (1961), water bodies with form number in the range of 0.25–1.5, classified as the mixed tide, predominantly semidiurnal, i.e. there are two high and two low tides per day with diurnal inequality. The maximum mean tidal range is observed in the ST3 during the spring tide that exceeded 4.25 m and reduced to about 2.2 m in the neap tide phase. The mean spring and neap tidal range varies between 2.53 and 1.25 m at ST1, and 3.73 and 1.89 m at ST2. The tidal range in ST3 that exceed 4 m at spring tide represents the highest tidal range observed in the entire Arabian Gulf beside approximately the same magnitude that recorded in Kuwait Bay (Alosairi et al. 2018).

Moreover, to assess the model accuracy, sea water level data in the base scenario are analyzed using harmonic analysis (Boon 2007), to find the main astronomical constituents and to examine the results in ST2 and ST3 as illustrated in the Table 2. The most accurate amplitude constituents were O_1, M_2, S_2, and K_1 in ST2 and ST3, respectively, with the relative differences between measured and simulated data are less than 10%, except for the N_2 which offer a relative difference reaches to 23%. The results of the harmonic analysis of measured data indicate that the phase difference for M_2, the main contributor constituent that governed the time of occurring high and low water, between ST2 and ST3 was about 12 degrees, i.e. the high water reaches to ST3 after about 25 min relative to ST2, and the model has reproduced this difference very well.

Tidal currents in KA and KZ have two distinguish directions, northwestward through the flood and southeastward during ebb tide as shown in Fig. 7. The results indicated

Table 2 Comparison of measured and simulated values of amplitudes and phases for principle tidal constituents

ST3				ST2				Tidal constituents
Phase (degree)		Amplitude (m)		Phase (degree)		Amplitude (m)		
Sim	Obs	Sim	Obs	Sim	Obs	Sim	Obs	
231.85	226.97	0.365	0.353	227.1	221.64	0.349	0.351	O_1
319.65	317.14	0.677	0.584	310.55	307.79	0.614	0.561	K_1
317.28	309.18	1.533	1.591	305.72	297.83	1.384	1.409	M_2
96.95	85.98	0.482	0.528	80.38	65.27	0.446	0.46	S_2
219.77	209.33	0.194	0.258	206.1	189.59	0.181	0.247	N_2

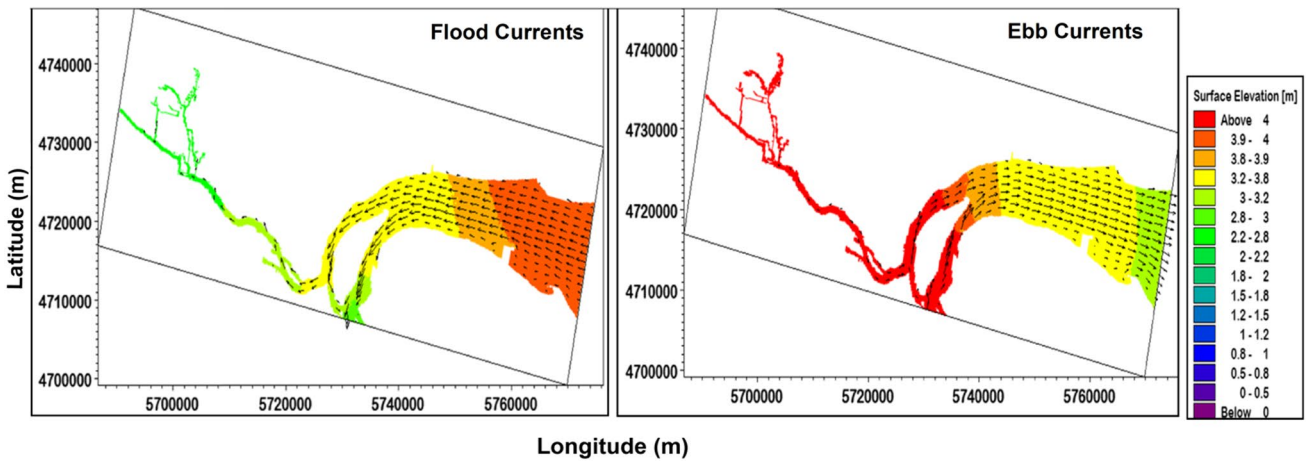

Fig. 7 Tidal currents direction through the flood and ebb phases (the black arrows represent the direction of tidal currents)

that the maximum springs-neap current velocity is ranged between 1.1 and 1.01 m/sec and, 1.472 and 1.16 m/sec in KA and KZ, respectively. Additionally, the ebb was longer than the flood period due to the tidal asymmetry resulting from the shallow water nature of the area, and hence flood currents were higher than ebb currents in the most locations in KA and KZ, and these results are consistent with the previous studies (Al-Ramadhan 1988; Al-Mahdi et al. 2009; Al-Mahdi and Mahmood 2010; Al-hasem 2018).

3.2 Changes in Amplitude and Phase of Principal Constituents

Generally, the effects of SLR on the tidal dynamics are more significant in shallow waters than in deep waters. Hence, since SLR increases the water depth, the amplitudes and phases of harmonic components of tides are sensitive to such changes and may display many variations in its propagation characteristics (Kuang et al. 2016). To investigate the possible changes in the amplitudes and phases of the five principles tidal components, five sites along the study area are chosen. The first station (KA1) located near Arabian Gulf north edge, the second (KA2) at the upper end of KA approximately, the third (KSh) situated at the middle of Khor Shytana, the forth (KZ1) located at Umm Qasar town, while the last one (KZ2) located at Khor Al-Zubair port as shown in Fig. 8.

The response of constituents' amplitude to SLR was a spatially non-uniform, with notable decrease and increase between different SLR scenarios. Figure 9 (left side) shows the responses of constituents' amplitudes to the different SLR scenarios. For M_2, there is a decrease in its amplitude as sea level increases except for the scenario of 0.25 m, which depicted a little increase at all sites except at the KA1 and KA2 stations, show a slight decrease in about of 0.1 cm. The maximum reduction in the M_2 amplitude occurs at KZ2, which was about 2 cm (1.5%) when SLR reaches 1 m compared to the base scenario. Similarly, S_2 response to SLR was irregular, with a notable increase in its amplitude in all locations along study area except at two sites, KA2, and KZ2 which shown a slight decrease with SLR scenarios. Moreover, there is an increase in N_2 amplitude in KA2, KSh, and KZ1 with SLR scenarios, while it offers a slight decrease at KZ2 with about 0.2 cm. On the other hand, for the diurnal constituents, K_1 displays a little increase in KA1 and KA2, whereas there is a reduction in its amplitude reaches about 1.2%, 3.9%, and 6.65% at KSh, KZ1, and KZ2, respectively. While O_1 was presented no noticeable change at KA1 and KA2 stations, whereas it is experiencing a linear decrease in its amplitude with SLR scenarios at rest locations, with the maximum decrease occurs at the KZ2, reaches to 4.9% when SLR reaches 1 m relative to the base scenario. However, as tidal wave propagates into shallow waters, the magnitude of the tidal changes is particularly sensitive to the bottom friction effects (Kumar and Balaji 2015). When sea level increases, the water depth increase also and leads to inundate new areas, as well as, the tidal flats are diminished, these two processes make the tidal systems subject to many variations due to the shallow water tidal wave characteristics. The difference in tidal response to SLR is usually attributed to a change in these two factors, the bottom friction coefficient and tidal flats, which affect the distribution of tidal wave energy and hence their different properties. Therefore, SLR can lead to an increase in the amplitude of harmonic constituents due to a decrease in the friction effect especially in a shallow water (Müller et al. 2011; Pickering et al. 2012; Pelling et al. 2013a, b), or a decrease in the amplitude of these constituents because of the increase of tidal energy dissipated by new inundated areas of the tidal flats which act as a source of wave energy dissipation (Ross et al. 2017). In the shallow

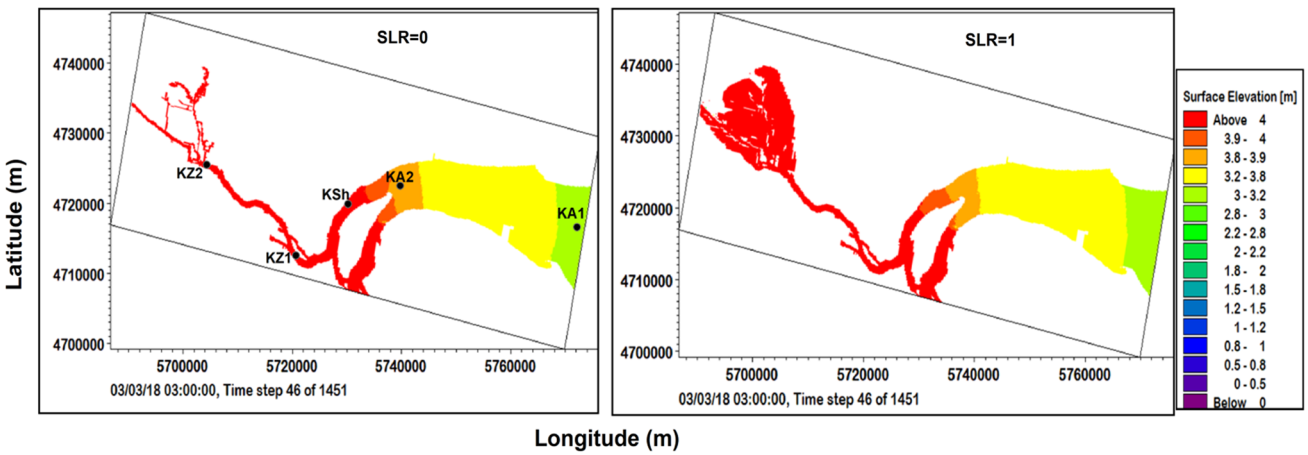

Fig. 8 Comparison between base scenario and SLR of 1 m

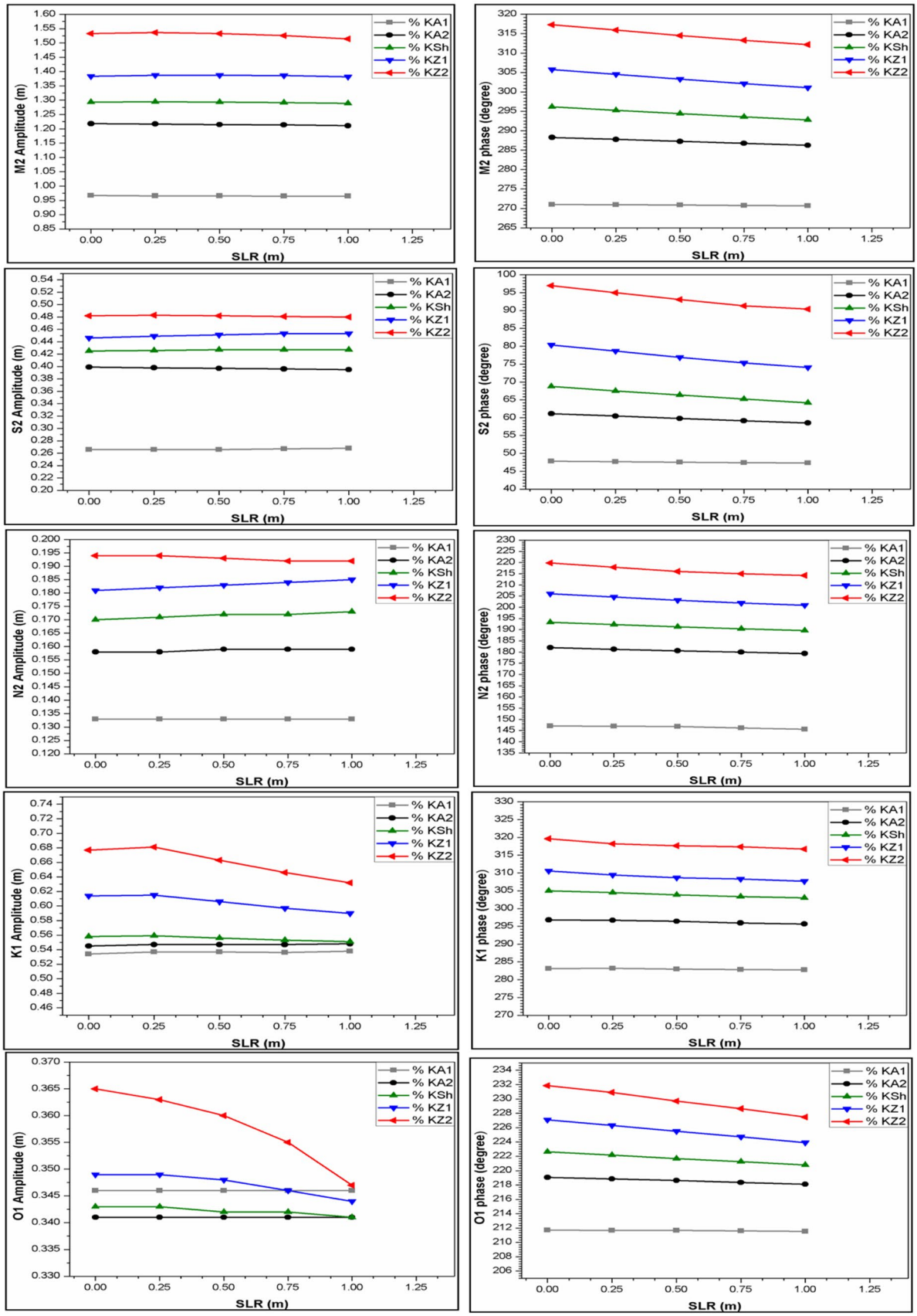

Fig. 9 Response of the amplitude of principle tidal constituents to SLR scenarios

water equations (Mike21), the effect of bottom friction is parameterized through the bed friction coefficient, which is inversely proportional to the depth (DHI 2007), and hence SLR increased water depth, so the amplitude of tidal waves is expected to increment as sea level rises due to the reduction of the tidal energy that dissipated by friction effects. In contrast, our results revealed that as sea level rising, there is a decreasing in the amplitudes of principle tidal constituents especially when tidal wave propagates further towards the upper reaches of KZ. However, the simulation result indicates that most of the tidal flats on both sides of KA and KZ are subjected to permanent inundation when sea level rises, as well as the whole upper reaches of KZ, undergoes to periodic flooding through the tidal cycle as shown in Fig. 8, so these newly inundated areas act the main source of tidal energy dissipation, and the reduction in tidal constituents amplitudes can be attributed to this effect. Consequently, the reduction in amplitudes of the tidal constituents leading to a decrease in tidal range, our results indicate that the mean spring range in KZ will decrease (1.3%) from 4.03 to 3.98 m, while the mean neap rang will decrease (2%) from 2.102 to 2.06 m when sea level rising by 1 m. The decreasing of the tidal range has many impacts on the vertical mixing processes, the decrease of tidal range will reduce the tidal mixing and a consequence many implications in biogeochemical processes and ecosystem stability (Hong and Shen 2012).

The tidal constituents' phase response to SLR is shown in Fig. 9 (right side), obviously there is a reduction in constituents' phases as sea level rises. The decrement in tidal constituents' phases indicates that the tidal waves will arrive earlier when sea level rises due to the nature of tidal wave propagation and their dependency on the depth, especially at shallow water bodies. The change in phase explains the time of tidal arrivalT, which can be estimated by (Kuang et al. 2016):

$$T = \frac{\Delta g}{360} \times T_{\text{const.}}, \tag{3}$$

where Δg is the phase variation and $T_{const.}$ is the period of the tidal constituent. However, for SLR of 1 m as an example, the semi-diurnal component M_2 (T_{M2}=12.42 h) (Boon 2013), moves from KA1 and arrives at KA2, KSh, KZ1, and KZ2 after 33.1, 45.5, 64.1, and 86.9 min compared to 35.1, 51.7, 70, 95.2 min at the base scenario. Similarly, the S_2 (T_{S2} = 12h) arrives earlier by 6, 8, 12, and 12 min, N_2 (T_{N2} = 12.69h) arrives earlier by 2.2, 7.2, 10.7, and 9.2 min, K_1 (T_{K1}=23.93 h) arrives earlier by 0.3, 4.7, 12, 8.5 min, and O_1 (T_{O1}=25.81 h) arrives earlier by 4.3, 8.6, 17.2, and 17.2 min to KA1, KSh, KZ1, and KZ2, respectively. However, the tidal wave speed in shallow water ($\sqrt{gd}$) depends on the water depth d, so SLR will lead to an increase in the tidal wave propagation. Consequently, the phases of tidal constituents decrease with SLR, which refer to early arrive of high and low water in the future.

3.3 Change in Tidal currents

The tidal currents play an important role in different aspects and represent the main factor responsible for the physical processes in the study area and working to keep the continuous exchange of water masses with the Arabian Gulf. However, the simulation results revealed that the effect of SLR on tidal currents is clearly spatially variable and different between flood and ebb currents. Figure 10 illustrates the variations in tidal currents magnitude and directions with SLR scenarios. For SLR of 1 m as an example, at KA1 station, there is a decrease in flood and ebb currents when sea-level increase, the decreasing ratio is 2.3% and 3.1% relative to the base scenario for flood and ebb currents, respectively. While at KA2 station, a little increase is observed in tidal currents with the increment ratio of 0.72% and 0.79% for flood and ebb currents, respectively. Furthermore, at KSh station, there is an increase in ebb currents reaches 9.35%, and a decrease in flood currents reaches 7.08%. Similarly, at KZ1 station there is an increase in ebb currents reaches about 7.63%, and a decrease in flood currents reaches 4.55%. Lastly, at KZ2 station, there is an increase in flood currents reaches about 6.6%, and an increase in ebb currents which increment by 6.61% when sea level rises by 0.5 m, then the increase ratio drops to reach about only 0.47% with SLR of 1 m. However, the simulation result indicates that there are no substantial variations in tidal currents directions, and it mostly stays unchanged when sea level rises, except for a slight varies which can be attributed to the time variations of the tidal wave propagation due to the increment of tidal wave celerity as water depth increases with SLR. Correspondingly, the increase of tidal wave speed leading to a minor shift in time of peak ebb and flood currents. Moreover, the simulation results show that the maximum tidal currents exist in the deeper parts of KA and KZ. Additionally, as shown in Fig. 10, there are little changes in tidal currents in KA1 and KA2 with SLR scenarios, which can be attributed to large cross-sections of KA. While the most variations in tidal currents occur at KSh, KZ1, and KZ2, respectively, due to a narrower channel at these locations which can concentrate the tidal energy and enhance the tidal currents velocities making it more sensitive to sea level rising.

4 Conclusions

The response of tidal dynamics to potential sea-level rise in Khor Abdulla and Khor Al-Zubair are studied by assuming several scenarios using the Mike21 model. The field

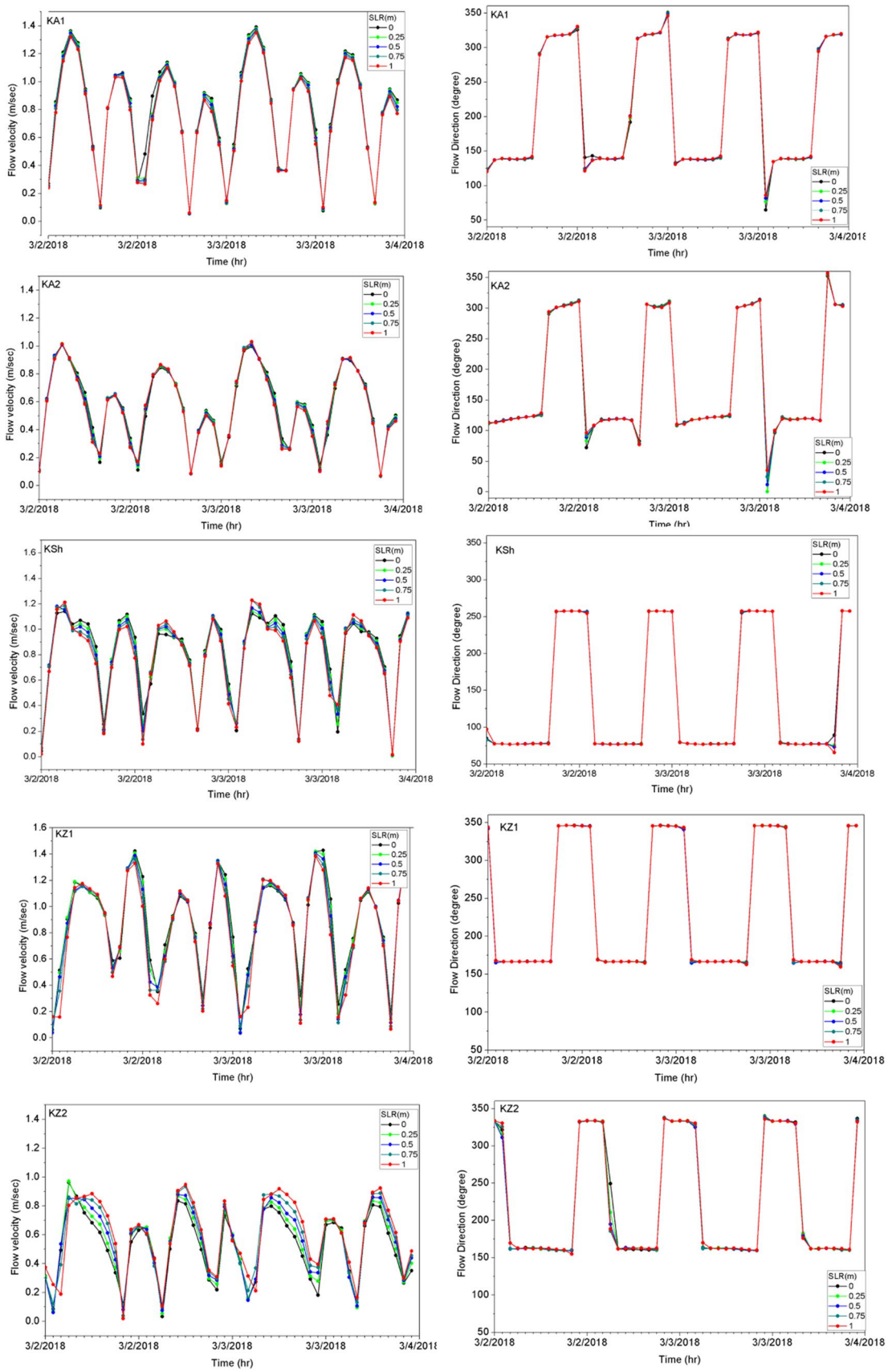

Fig. 10 Response of the tidal currents to SLR scenarios

measurements of water level and currents velocity are used in the calibration and validation of the model results for the base scenario. The result of simulations and measurement indicate that there are asymmetries in the tidal wave that propagates farther in inland direction with a gradual increase in their amplitude and hence in its tidal range. However, the simulation results showed that the response of tidal constituents to potential SLR scenarios is spatially nonuniform and shows non-linear responses. The M_2 amplitude experience a notable decrease as sea level rises more than 0.25 m, the most reduction occurs at KZ2 which located in the upper reaches of the study area. While S_2 and N_2 amplitudes exhibit a little increase with SLR scenarios in most locations along KA and KZ. Moreover, K_1 and O_1 amplitudes approximately display a linear reduction as sea level rises. Consequently, the reduction in amplitudes of the tidal constituents leading to a decrease in tidal range, the decreasing of the tidal range has many impacts on the vertical mixing processes and a consequence many implications in biogeochemical processes and ecosystem stability. Furthermore, the phase of the constituents experiences a linear decrease when sea level rises, which implies that these waves will propagate faster in the future. The tidal currents also imply a spatially irregular response to SLR with a notable shift in the time of peak flood and ebb currents velocities, especially in KZ. The results provide useful information and will be significant in the future assessments of coastal developments in this region.

Acknowledgements The authors are grateful to DANIDA (the Danish International Development Agency) for providing the Mike Software. Additionally, special thanks are given to the technician teams of, General Company for Ports of Iraqi (GCPI), and Marine Science Center/ University of Basrah for their help in the field measurements. The authors also would like to thank Daewoo Engineering and constructing company for providing valuable data in this region.

Compliance with Ethical Standards

Conflict of Interest The authors declare that they have no conflict of interest.

References

Al-hasem AM (2018) Tidal current behaviors and remarkable bathymetric change in the South-Western part of Khor Abdullah, Kuwait. Int J Mar Environ Sci 12(2):118–125

Al-Mahdi AA, Abdullah SS, Husain NA (2009) Some features of the physical oceanography in Iraqi marine water. Mesop J Mar Sci 24:13–24

Al-Mahdi AA, Mahmood AB (2010) Some features of tidal currents in Khor Abdullah, North West Arabian Gulf. J Mar Sci King Abdul Al-Aziz Univ 21(1):162–182

Al-Mahmood HK, Mahmood AB, Al Mola TJ (2018) Scenarios of Mean Sea-level rise and their impacts on Iraqi coast. Arab Gulf J., vol. under pres.

Alosairi Y, Pokavanich T, Alsulaiman N (2018) Three-dimensional hydrodynamic modelling study of reverse estuarine circulation: Kuwait Bay. Mar Pollut Bull 127:82–96

Alothman A, Ayhan M (2010) Dtection of sea level rise within the Arabian Gulf using space based GNSS measurements and insitu Tide Gauge data. In: 38th COSPAR Scientific Assembly, vol 38, p 3

Alothman AO, Bos MS, Fernandes RMS, Ayhan ME (2014) Sea level rise in the north-western part of the Arabian Gulf. J Geodyn 81:105–110

Al-Ramadhan BM (1988) Residual fluxes of water in an estuarine lagoon. Estuar Coast Shelf Sci 26(3):319–330

Alsahli MM, Al-hasem AM (2016) Vulnerability of Kuwait coast to sea level rise. Geogr Tidsskr J Geogr 116(1):56–70

Arns A, Wahl T, Dangendorf S, Jensen J (2015) The impact of sea level rise on storm surge water levels in the northern part of the German Bight. Coast Eng 96:118–131

Boon JD (2007) World tides user manual v1.03, USA, p 25

Boon JD (2013) Secrets of the tide: tide and tidal current analysis and predictions, storm surges and sea level trends. Elsevier, Amsterdam, p 224

Carless SJ, Green JAM, Pelling HE, Wilmes SB (2016) Effects of future sea-level rise on tidal processes on the Patagonian Shelf. J Mar Syst 163:113–124

Church JA, White NJ (2006) A 20th century acceleration in global sea-level rise. Geophys Res Lett 33(1):L01602

Church JA, White NJ (2011) Sea-level rise from the late 19th to the early 21st century. Surv Geophys 32(4–5):585–602

Defant A (1961) Physical oceanography, vol 1. Pergamon, London, p 729

DHI (2007) Scientific documentation, MIKE 21 hydrodynamic Module, DHI water and environment. DHI Software Horsholm, Denmark

Du J, Shen J, Zhang YJ, Ye F, Liu Z, Wang Z, Wang YP, Yu X, Sisson M, Wang HV (2018) Tidal response to sea-level rise in different types of estuaries: the importance of length, bathymetry, and geometry. Geophys Res Lett 45(1):227–235

Filipova V, Aruna R, Prasoon S (2012) Urban flooding in Gothenburg-A Mike 21 study. J Water Manag Res 68:175–184

Gong Z, Zhang C, Wan L, Zuo J (2012) Tidal level response to sea-level rise in the Yangtze estuary. China Ocean Eng 26(1):109–122

Haines P (2008) Anticipated response of coastal lagoons to sea level rise. In: National conference on climate change: responding to sea level rise. IPWEA, Coffs Harbour, Australia

Harker A, Green JAM, Schindelegger M (2019) The impact of sea-level rise on tidal characteristics around Australia. Ocean Sci 15(1):147–159

Hong B, Shen J (2012) Responses of estuarine salinity and transport processes to potential future sea-level rise in the Chesapeake Bay. Estuar Coast Shelf Sci 104–105:33–45

IPCC (2007) Climate change 2007: working group i: the physical science basis, contribution of working group i to the fourth assessment report of the intergovernmental panel on climate change

IPCC (2013) Climate change : the physical science basis: working group i contribution to the fifth assessment report of the intergovernmental panel on climate change. Cambridge University Press, Cambridge

Kuang C, Chen W, Gu J, Zhu DZ, He L, Huang H (2014) Numerical assessment of the impacts of potential future sea-level rise on hydrodynamics of the Yangtze River Estuary, China. J Coast Res 295(3):586–597

Kuang C, LiangH MaoX, KarneyB GuJ, HuangH ChenW, Song H (2016) Influence of potential future sea-level rise on tides in the China Sea. J Coast Res 331:105–117

Kumar SS, Balaji R (2015) Effect of bottom friction on tidal hydrodynamics along Gulf of Khambhat, India. Estuar Coast Shelf Sci 154:129–136

Lafta AA, Al-Aeaswi QMF, Al-Taei SAR (2013) Total dissolved solids modeling in the Shatt Al-Basrah canal, using Mike 11. Mesop J Mar Sci 28(2):139–150

Li Y, Zhang H, Tang C, Zou T, Jiang D (2016) Influence of rising sea level on tidal dynamics in the Bohai Sea. J Coast Res 74:22–31

Mengel M, Levermann A, Frieler K, Robinson A, Marzeion B, Winkelmann R (2016) Future sea level rise constrained by observations and long-term commitment. Proc Natl Acad Sci 113(10):2597–2602

Mohamed ARM, Ali TS, Hussain NA (2002) The physical oceanography and fisheries of Iraqi marine waters, Northwest Arabian Gulf, pp 47–56. In: Proceedings on utilization of marine resources regional seminar organized jointly by Islamic Education Scientific and Cultural Organization (ISESCO) and National Institute of Oceanography (NIO), pp 20–22

Al-Faw Grand Port Marine Survey, Report Conducted by Marine Science Center/Basrah University to General Company Of Iraq Ports (unpublished report)

Müller M, Arbic BK, Mitrovica JX (2011) Secular trends in ocean tides: observations and model results. J Geophys Res Ocean 116(C5013):1–19

Nash JE, Sutcliffe JV (1970) River flow forecasting through conceptual models part I: a discussion of principles. J Hydrol 10(3):282–290

Nerem RS, Beckley BD, Fasullo JT, Hamlington BD, Masters D, Mitchum GT (2018) Climate-change–driven accelerated sea-level rise detected in the altimeter era. Proc Natl Acad Sci 115(9):2022–2025

Nicholls RJ, Marinova N, Lowe JA, Brown S, Vellinga P, De Gusmao D, Hinkel J, Tol RSJ (2011) Sea-level rise and its possible impacts given a 'beyond 4 degrees C world' in the twenty-first century. Philos Trans R Soc A Math Phys Eng Sci 369:161–181

Passeri DL, Hagen SC, Plant NG, Bilskie MV, Medeiros SC, Alizad K (2016) Tidal hydrodynamics under future sea level rise and coastal morphology in the Northern Gulf of Mexico. Earth's Future 4(5):159–176

Pelling HE, Green JAM (2013) Sea level rise and tidal power plants in the Gulf of Maine. J Geophys Res Ocean 118(6):2863–2873

Pelling HE, Green JAM, Ward SL (2013a) Modelling tides and sea-level rise: to flood or not to flood. Ocean Model 63:21–29

Pelling HE, Uehara K, Green JAM (2013b) The impact of rapid coastline changes and sea level rise on the tides in the Bohai Sea, China. J Geophys Res Ocean 118(7):3462–3472

Pickering MD, Wells NC, Horsburgh KJ, Green JAM (2012) The impact of future sea-level rise on the European Shelf tides. Cont Shelf Res 35:1–15

Ross AC, Najjar RG, Li M, Lee SB, Zhang F, Liu W (2017) Fingerprints of sea level rise on changing tides in the Chesapeake and Delaware Bays. J Geophys Res Ocean 122(10):8102–8125

Shahidi AE, Rohani MS, Parsa J, Lemckert C (2015) Effects of sea level rise on the salinity of Bahmanshir estuary. Int J Environ Sci Technol 12(10):3329–3340

Siddig NA, Al-Subhi AM, Alsaafani MA (2019) Tide and mean sea level trend in the west coast of the Arabian Gulf from tide gauges and multi-missions satellite altimeter. Oceanologia 61:401–411

Siqueira BVP (2011) Climate change impacts on mixing and circulation at Songkhla Lagoon, Thailand. MSc Thesis. TU Delft

SOC (2014) Common seawater supply project,high priority survey, bathymetry survey report and drawings, report introduced by Tatweer LTD to South Oil Company, Iraq (Unpublished Report)

Sriver RL, Urban NM, Olson R, Keller K (2012) Toward a physically plausible upper bound of sea-level rise projections. Clim Change 115(3–4):893–902

Suh SW (2016) Tidal asymmetry and energy variation due to sea-level rise in a macro tidal bay. J Coast Res 75(sp1):765–770

Sultan SAR, Ahmad F, Elghribi NM, Al-Subhi AM (1995) An analysis of Arabian Gulf monthly mean sea level. Cont Shelf Res 15(11–12):1471–1482

Sultan SAR, Moamar MO, El-Ghribi NM, Williams R (2000) Sea level changes along the Saudi coast of the Arabian Gulf. Indian J Mar Sci 29(3):191–200

Surya MY, He Z, Xia Y, Li L (2019) Impacts of sea level rise and river discharge on the hydrodynamics characteristics of Jakarta Bay (Indonesia). Water 11(7):1384

Testuta L, Duvata V, Ballua V, Fernandesc R, Pougeta F, Salmona C, Dyment J (2016) Shoreline changes in a rising sea level context: the example of Grande Glorieuse, Scattered Islands, Western Indian Ocean. Acta Oecol 72:110–119

Valentim JM, Vaz L, Vaz N, Silva H, Duarte B, Caçador I, Dias JM (2013) Sea level rise impact in residual circulation in Tagus estuary and Ria de Aveiro lagoon. J Coast Res 65(sp2):1981–1986

Wernberg T, Russell BD, Thomsen MS, Connell SD (2014) Marine biodiversity and climate change. Glob Environ Change 181–187

Woodworth PL, Teferle FN, Bingley RM, Shennan I, Williams SDP (2009) Trends in UK mean sea level revisited. Geophys J Int 176(1):19–30

Xie Y, Lv X, Liu R, Mao L, Liu X (2015) Research on port ecological suitability evaluation index system and evaluation model. Front Struct Civ Eng 9(1):65–70

Zakaria S, Al-Ansari N, Knutsson S (2013) Historical and future climatic change scenarios for temperature and rainfall for Iraq. J Civ Eng Archit 7(12):1574–1594